Original Article

Comparative transcriptome analysis of transcultured human skin-derived precursors (tSKPs) from adherent monolayer culture system and tSKPs-derived fibroblasts (tFBs) by RNA-Seq

Ru Dai[1,2,§], Wei Chen[3,§], Wei Hua[1], Lidan Xiong[1], Yiming Li[1], Li Li[1,*]

[1] Department of Dermatology, West China Hospital, Sichuan University, Chengdu, Sichuan, China;
[2] Department of Dermatology, Ningbo First Hospital, Ningbo University, Ningbo, Zhejiang, China;
[3] Department of Medical Cosmetology, The Second People's Hospital of Chengdu, Chengdu, Sichuan, China.

SUMMARY   Transcultured human skin derived precursors (tSKPs) from adherent monolayer culture system have similar characteristics as traditional skin derived precursors (SKPs), making tSKPs a suitable candidate for regenerative medicine. tSKPs can differentiate into fibroblasts. However, little is known about the molecular mechanism of the transition from tSKPs to fibroblasts. Here, we compared the transcriptional profiles of human tSKPs and tSKPs-derived fibroblasts (tFBs) by RNA-Sequence aiming to determine the candidate genes and pathways involving in the differentiation process. A total of 1042 differentially expressed genes (DEGs) were identified between tSKPs and tFBs, with 490 genes up-regulated and 552 genes down-regulated. Our study showed that these DEGs were significantly enriched in tumor necrosis factor signaling pathway, focal adhesion, extracellular matrix-receptor interaction and phosphatidylinositol 3 kinase (PI3K)/protein kinase B (Akt) signaling pathway. A further transcription factors (TFs) analysis of DEGs revealed the significantly down-expressed TFs (p21, Foxo1and Foxc1) in tFBs were mostly the downstream nodes of PI3K-Akt signaling pathway, which suggested PI3K-Akt signaling pathway might play an important role in tSKPs differentiation. The results of our study are useful for investigating the molecular mechanisms in tSKPs differentiation into tFBs, making it possible to take advantage of their potential application in regenerative medicine.

Keywords   skin derived precursors, fibroblasts, stem cell, RNA-Seq, adherent culture system

1. Introduction

Skin-derived precursors (SKPs) from dermis, firstly described by Toma *et al.* in 2001 (*1*), are adult stem cells with the capacities of self-renewal and multipotency (*2*). Conventionally, SKPs are cultured as floating spheres in suspending serum-free medium with required growth factors (*3*); however, many studies have reported that isolating human SKPs by this protocol has many limitations such as relatively low yield (*4*), slow growth rate (*3*), and heterogeneous spheres (*5*). Therefore, it is unsurprising that several studies have demonstrated a new technique to transculture human SKPs from adherent monolayer culture system (henceforth termed tSKPs), and these tSKPs are similar to traditional SKPs in morphology and function (*6-8*). Developments in tSKPs research have indicated their potential application in regenerative medicine.

Under proper stimulus, tSKPs can differentiate into cells of both neural and mesodermal lineages, including neurons (*7*), Schwann cells (*6,7*), smooth muscle cells (*6,8*), osteogenic (*6,7*) and adipogenic cells (*6,7*). It has also been reported that tSKPs can differentiate into fibroblasts (FBs) (*8*). Cultured in low-glucose medium with 15% fetal bovine serum, tSKPs presented fibroblast-like morphology and expressed fibroblast marker of prolyl-4-hydroxylase beta-an enzyme involved in collagen synthesis (*8*). Previous studies have demonstrated that SKPs became morphologically similar to the endogenous fibroblasts and expressed fibroblast markers when transplanted into dermis, while did not express markers of neurons or peripheral glia (*9,10*). Moreover, SKPs could integrate throughout the thickness of the dermis, mostly locating in the dermal papilla and dermal sheath of hair follicles (*9*). As the principal cellular target of skin regeneration, FBs play a pivotal role in maintaining the morphology and function of normal skin. Since tSKPs can differentiate

into fibroblasts, they may serve as potential sources for treating aged skin, atrophic skin diseases or skin repair by replenishing the lost or damaged FBs.

As a requisite to potential applications in cell-based therapies, it is essential to understand the molecular mechanisms that why and how tSKPs can differentiate into FBs. Actually, any biological changes of stem cells including whether they self-renew, remain quiescence, proliferate, differentiate or undergo apoptosis, is ultimately the alterations of gene expression (*11*). Therefore, it is necessary to investigate gene evolution of related cells at the expression level for which may provide further insights into mechanisms.

To date, no studies have compared the transcriptomic profiles between human tSKPs and tSKPs-derived FBs (tFBs). Hence, this study aims to perform a comparative transcriptomes between tSKPs and tFBs by RNA-Sequence (RNA-Seq). We assume that our study may help determine the candidate genes and pathways that involve in the differentiation of tSKPs to fibroblasts, thus broaden the potential application of tSKPs in the treatment of skin-related diseases.

2. Materials and Methods

2.1. Cell Preparation

Human skin samples were collected from patients undergoing circumcisions with informed consents signed. Our study was conducted in accordance with the ethical guidelines of West China Hospital (Chengdu, China) and had Ethics Committee approval (No. 2017064A).

The protocol for isolating tSKPs has been described previously in our study (*6*). For directing tSKPs into tFBs, spheres were collected, resuspended in dulbecco's modified eagle medium (DMEM) containing 10% fetal bovine serum, and then seeded into cell culture dishes.

2.2. Immunocytochemistry

Cells were plated onto slides and fixed with 4% paraformaldehyde for 30 minutes at room temperature. The fixed cells were permeabilized with 0.25% Triton X-100 for 10 minutes and subsequently blocked with 3% bull serum albumin for 30 minutes. Then, cells were incubated with primary antibodies overnight at 4℃ and with secondary antibodies for 1 hour at room temperature. Finally, cells were incubated with DAPI (Dojindo, Japan) for 1 minute before visualizing under a fluorescence microscope (Olympus, Japan). Primary antibodies were anti-Versican (Abcam, UK, 1:200), anti-Fibronectin (Abcam, UK, 1:250), anti-Collagen I (Abcam, UK, 1:250), anti-Vimentin (Abcam, UK, 1:250), anti-Sox2 (Abcam, UK, 1:250) and anti-Nestin (Abcam, UK, 1:250). The secondary antibodies were Alexa Fluro[®] 488 donkey anti-mouse IgG (Abcam, UK, 1:500) and Alexa Fluro[®] 488 goat anti-rabbit IgG (Abcam, UK,

1:500). The protocol was performed in triplicate for each cell type described.

2.3. RNA-Seq

2.3.1. Library Preparation

cDNA library preparation was prepared at Novogene Co., LTD, Beijing. Total RNA was extracted from samples by Trizol (Ambion, USA). mRNA was purified using olidgo (dT) magnetic beads, and broken into short fragments in fragmentation buffer. Taking mRNA as a temple, first strand cDNA was synthesized using random hexamers. Second strand cDNA was subsequently synthesized in the condition of deoxyribonucleoside triphosphates (dNTPs), DNA polymerase I, and buffer. cDNA was purified with AMPure XP beads and then performed end reparation and 3'-end single nucleotide A addition. At last, the resulting fragments were screened by AMPure XP beads and enriched by PCR amplication. The quality of library products was determined on the Agilent Bioanalyzer 2100 system, and the qualified products were used for sequencing on Illumina HiSeq™ 2000.

2.3.2. Mapping Reads to the Reference Genome

The original image data generated from HiSeq was transferred into sequence using base calling, and these sequences were defined as "raw reads". The resulting sequences were filtered as follows: remove adaptor sequences, N sequences and low-quality sequences. The remaining reads were mapped to the human genome using Tophat v2.0.12, and no more than 2 mismatches were allowed in the alignment. The RNA-Seq data is provided on GEO with the accession number of GSE133190.

2.3.3. Statistical Analysis and Screening of Differentially Expressed Genes (DEGs)

The gene expression level was presented by the Reads Per Kb per Million reads (RPKM) method, which was calculated based on the length of the gene and sequencing discrepancies. HTSeq v0.6.1 was used to count the read numbers mapped to each gene. RPKM values could be used for comparing the difference of gene expression in different samples using DEGSeq v1.12.0. *p*-value was used corresponding to a differential gene expression test at statistically significant levels. "|log2 (Fold change)| ≥ 1 and False Discovery rate < 0.001" were set to identify DEGs as the threshold.

2.3.4. Functional Annotation of DEGs

Gene ontology (GO) enrichment analysis of DEGs that were significantly enriched in all GO terms compared

to genome background using GOSeq (Release 2.23). The corresponding biological functions related to the DEGs were also presented. The calculated *p* value was adjusted through Benjamini and Hochberg's approach, using an adjusted $p < 0.05$ as a threshold. GO terms with adjusted $p < 0.5$ were regarded as significantly enriched by DEGs.

The analysis of kyoto encyclopedia of genes and genomes (KEGG) was the major public pathway-related database, which provided all KEGG pathways that are significantly enriched in DEGs. The calculating formula was the same as that in GO analysis, using KOBAS v2.0.

The regulation of gene transcription, which is important for many biological functions, relies largely on transcription factors (TFs). TFs can active or inhibit downstream gene transcription by binding to specific upstream nucleotide sequences. TFCat (*http://www. tfcat.ca/*) is a curated catalog of mouse and human TFs based on a reliable core collection of annotation obtained by expert review of the scientific literature (*12*), which provides reliable data of functional category and confidence level of candidate TFs. In this study, TFCat was used to characterize and annotate TFs in DEGs.

2.4. Quantitative Real Time Reverse Transcription PCR (qRT-PCR) for Validation

Main DEGs involved in important KEGG pathways or related to TFs were selected to verify the RNA-Seq data by qRT-PCR: Mmp9, Ccl20, Vcam1, Csf3, Cxcl5, Foxo1, Nr4a1, Foxc1, Foxm1, Cited2, Mylk, Thbs1, Hmgb2, Dhcr24, Dhcr7 and Vegfc. Total RNA was extracted from cells using Trizol, then was converted to cDNA using the iScript™ cDNA Synthesis Kit (Bio-Rad, USA) according to the manufacturer's instructions. qRT-PCR was carried out using the CFX Connect™ Real-Time PCR Detection System (Bio-Rad, USA) with SsoAdvanced™ Universal SYBR® Green Supermix (Bio-Rad, USA). The primers were described in Table S1 (*http://www.biosciencetrends.com/action/ getSupplementalData.php?ID=63*). The mRNA expression levels were normalized by the internal β-actin control and the relative expression of each gene was calculated using the $2^{-\Delta\Delta Ct}$ method. Three independent biological experiments and two technical replicate were performed. Pearson correlation coefficient between qRT-PCR data and RNA-Seq data was calculated to validate RNA-Seq experiments.

3. Results

### 3.1. Differentiation of tSKPs into Fibroblasts

tSKPs were successfully isolated from primary adherent monolayer culture system established from human skin tissue. The tSKPs demonstrated a sphere-like structure in suspension 7 days after transculturing (Figure 1A). Being cultured in the medium differentiated toward tFBs, cells adhered to the plastic and presented a flattened and spindle-shaped morphology (Figure 1B), similar to the characteristic morphology of primary-cultured FBs (pFBs) (Figure 1C).
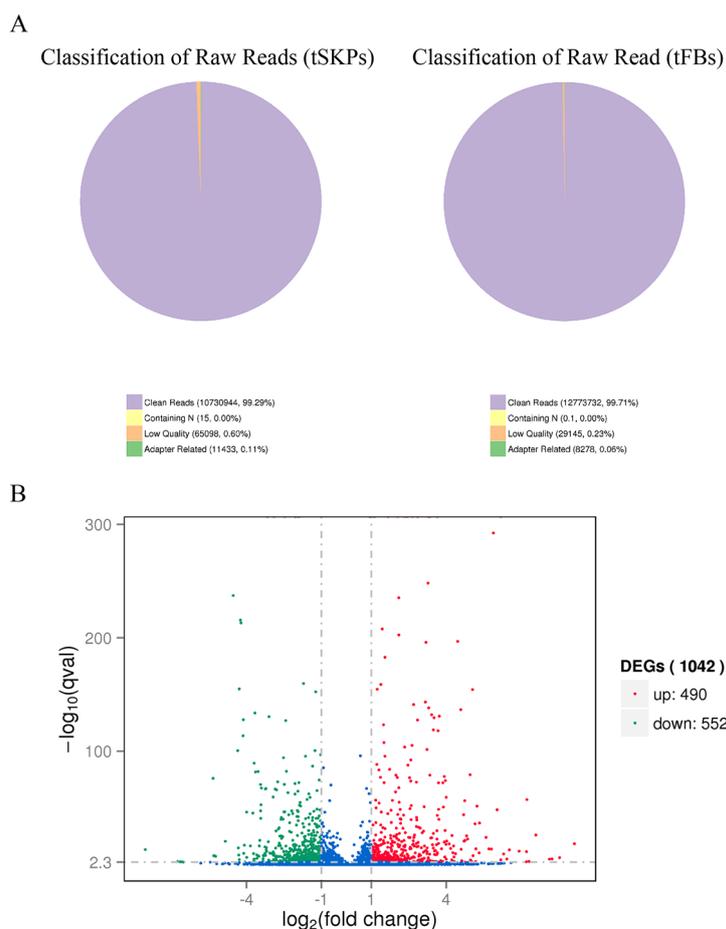
The protein expressions of cells were analyzed by immunocytochemistry. As shown in Figure 2, tSKPs expressed Versican (Figure 2A), Fibronectin (Figure 2D), Vimentin (Figure 2J), Sox2 (Figure 2M) and Nestin (Figure 2P), while did not express Collagen I (Figure 2G), which was consistent with traditional
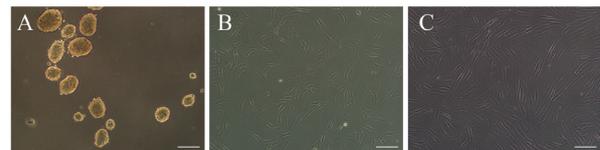
Figure 1. Morphology of tSKPs and fibroblasts. (**A**) tSKPs presented a sphere-like structure. (**B**) tFBs differentiated from tSKPs had same morphology as pFBs. (**C**) pFBs presented a flattened and spindle-shaped morphology. Scar bars: 100 μm.
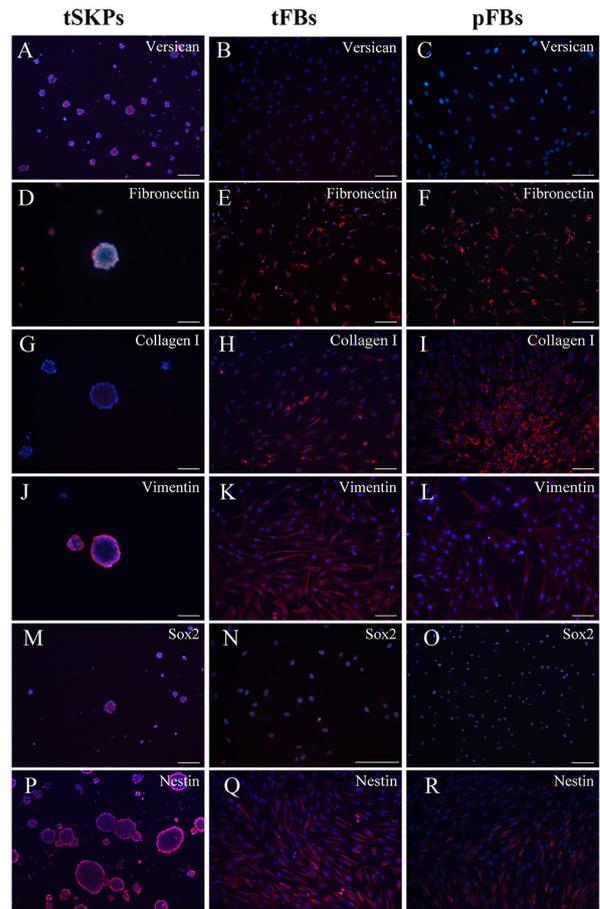
Figure 2. Immunocytochemical analysis of tSKPs and fibroblasts. tSKPs spheres expressed Versican (**A**), Fibronectin (**D**), Vimentin (**J**), Sox2 (**M**) and Nestin (**P**), did not express Collagen I (**G**); tFBs expressed Fibronectin (**E**), Collagen I (**H**), Vimentin (**K**) and Nestin (**Q**), did not express Versican (**B**) and Sox2 (**N**). PFBs expressed Fibronectin (**F**), Collagen I (**I**) and Vimentin (**L**), weakly expressed nestin (**R**), and did not express Sox2 (**O**) and Versican (**C**). Scar bars: 100 μm.

A

Classification of Raw Reads (tSKPs)   Classification of Raw Read (tFBs)

Clean Reads (10730944, 99.29%)
Containing N (15, 0.00%)
Low Quality (65098, 0.60%)
Adapter Related (11433, 0.11%)

Clean Reads (12773732, 99.71%)
Containing N (0.1, 0.00%)
Low Quality (29145, 0.23%)
Adapter Related (8278, 0.06%)

B

DEGs (1042)
up: 490
down: 552

Figure 3. Quality assessment of reads and DEGs between tSKPs and tFBs. (**A**) Classification of raw reads in tSKPs and tFBs. (**B**) Scattered plot of DEGs identified between tSKPs and tFBs.

Table 1. Summary of mapping results (mapping to reference genes)

Sample name	Total reads	Total mapped	Multiple mapped	Uniquely mapped	Non-splice reads	Splice reads
tSKPs_RNA	10730944	10389834 (96.82%)	600661 (5.6%)	9789173 (91.22%)	7759368 (72.31%)	2029805 (18.92%)
tFBs_RNA	12773732	12522653 (98.03%)	668801 (5.24%)	11853852 (92.8%)	9627457 (75.37%)	2226395 (17.43%)

tSKPs: transcultured skin-derived precursors; tFB: tSKPs-derived fibroblasts.

SKPs (*4*). tFBs expressed Fibronectin (Figure 2E), Collagen I (Figure 2H), Vimentin (Figure 2K), and Nestin (Figure 2Q), while were negative for Versican (Figure 2B) and Sox2 (Figure 2N). As for pFBs, they were positive for Fibronectin (Figure 2F), Collagen I (Figure 2I), Vimentin (Figure 2L) and Nestin (Figure 2R). However, the expression level of Collagen I was stronger and the Nestin expression level was weaker in pFBs compared with tFBs. pFBs also did not express Versican (Figure 2C) and Sox2 (Figure 2O). The results of immunofluorescence staining of tFBs and pFBs were similar. Herein, our data showed that tSKPs could differentiate into fibroblast in adhesive culture with serum, which was consistent with previous studies on mouse (*13*), and porcine (*14*). Concomitantly, they gradually lost the neural potential while appeared certain mesodermal capacity during this process.

3.2. Quality Assessment of Samples by RNA-Seq

More than 10 million raw reads were generated from tSKPs or tFBs. The percentage of clean reads of each library was 99.29% and 99.71% respectively (Figure 3A). The mapping rate of each one was 96.82% and 98.03% of the total read (Table 1). The detailed information of quality assessment of reads and statistics of alignment were presented in Figure 3A and Table 1.

3.3. Analysis of DEGs between tSKPs and tFBs

A total of 1042 DEGs were identified between tSKPs and tFBs, with 490 genes up-regulated and 552 genes down-regulated (Figure 3B). The full lists of up-regulated and down-regulated DEGs were shown in Table S2 (*http://www.biosciencetrends.com/action/*
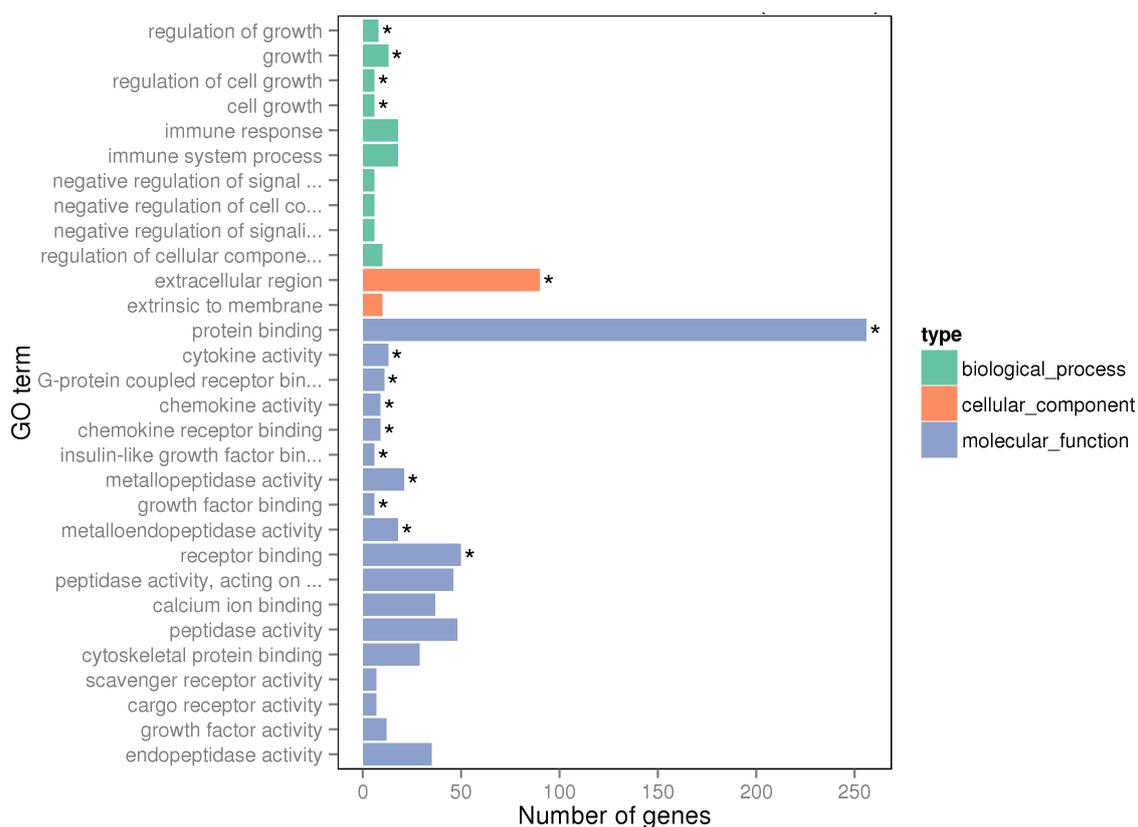
Figure 4. GO terms of DEGs. The top 30 enriched GO terms in the three main domains: biological process (10), cellular component (2), and molecular function (18). *Significantly enriched GO term.

getSupplementalData.php?ID=63).

3.4. GO Enrichment Analysis of DEGs

The 1042 DEGs could be categorized into 1971 GO terms. GO functional analysis identified the top 30 DEGs enriched GO terms (Figure 4). Among the GO annotations, 18 GO terms were in the domain of molecular function, and terms protein binding, cytokine activity, G-protein coupled receptor binding, chemokine activity, chemokine receptor binding, insulin-like growth factor binding, metallopeptidase activity, growth factor binding, metalloendopepetidase activity and receptor binding were dominant; 2 GO terms were in the domain of cellular component, and the term extracellular region was significantly enriched; 10 GO terms were related to biologic process, and the terms regulation of growth, growth, regulation of cell growth and cell growth were also significantly enriched.

3.5. KEGG Enrichment Analysis of DEGs

KEGG analysis identifies the pathways where DEGs are significantly enriched, which is beneficial for further understanding of DEGs biological functions. In our study, the top 20 enriched KEGG pathways were presented in Figure 5, and 9 pathways were identified to be significantly enriched in DEGs between tSKPs

and FBs (Table S3, *http://www.biosciencetrends.com/action/getSupplementalData.php?ID=63*), including tumor necrosis factor (TNF) signaling pathway (Figure S1, *http://www.biosciencetrends.com/action/getSupplementalData.php?ID=63*), focal adhesion (Figure S2, *http://www.biosciencetrends.com/action/getSupplementalData.php?ID=63*), extracellular matrix (ECM)-receptor interaction (Figure S3, *http://www.biosciencetrends.com/action/getSupplementalData.php?ID=63*) and phosphatidylinositol 3 kinase (PI3K)-protein kinase B (Akt) signaling pathway (Figure S4, *http://www.biosciencetrends.com/action/getSupplementalData.php?ID=63*). The main DEGs involved in these signaling pathways were listed in Table 2.

3.6. TF Annotation Analysis of DEGs

Regulation at the transcriptional level is important for gene expression. TFs can bind to specific upstream nucleotide sequences, thereby controlling the rate of transcription of downstream genes (*15*). Their activity determines how cells function and respond to external environments. The annotation analysis of TFs identified the differentially expressed TFs of DEGs between tSKPs and tFBs, and the main up-regulated and down-regulated TFs with strong evidence and their function were listed in Table 3.
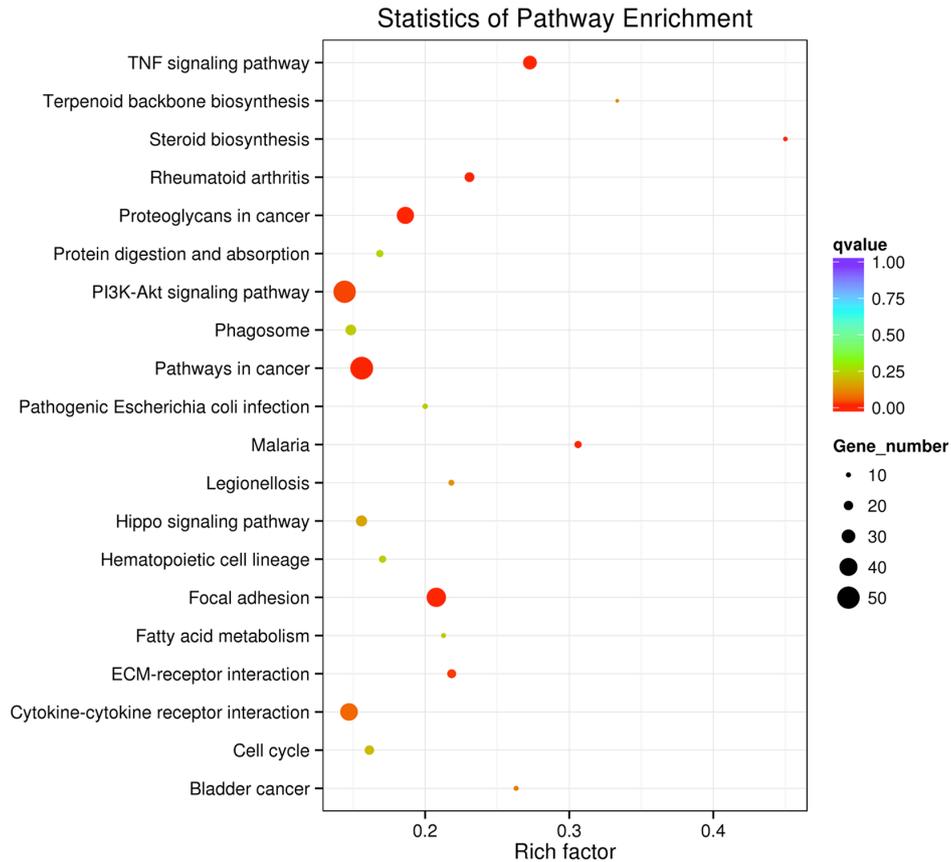
Figure 5. KEGG analysis of DEGs. Scattered plot of DEGs enriched KEGG pathways.

Table 2. List of possible signaling pathways and major DEGs involved in these pathways

Items	Up-regulated DEGs	Down-regulated DEGs
TNF signaling pathway	MMP9, CCL5/20, VCAM1, LIF, TNFAIP3, CXCL1/2/3/5, BIRC3, PTGSZ, IL18R1, IL6, IL1B	CREB3L1, VEGFC, CSF1
Focal adhesion	LAMC2/3, HGF, VEGFA, BIRC3, COL4A1, SHC2	MYLK, MYL9, FLNC, DAPK2, VEGFC, THBS1, ACTB, ITGA4, FLT1
ECM-receptor interaction	LAMC2/3, COL4A2/1, COL5A3, COMP, COL3A1	SDC1, THBS1, ITGA4
PI3K-Akt signaling pathway	LAMC2/3, BCL2L11, IL6, COMP, NGFR, COL4A1, CSF3	FGF1/5, CREB3L1, EPHA2, VEGFC, THBS1, ITGA4, FLT1, Itga6, Angpt1, Csf1, Il7r

DEGs: differentially expressed genes; TNF: tumor necrosis factor; ECM: extracellular matrix; PI3K: phosphatidylinositol 3 kinase; Akt: protein kinase B.

Table 3. List of major up-regulated and down-regulated transcription factors with strong evidence

Function	Up-regulated transcription factor	Down-regulated transcription factor
DNA binding	Snail2, Foxc1, Nfkb2, Xbp1, Mef2d, Cdkn1a, Nr1d1, Creg1, Foxo1, Nr4a2, Klf10, Tgif1	Foxm1, Hic1, Nr2f2, Tead1
Transactivation	Foxc1, Notch3, Xbp1, Mef2d, Foxo1, Nr4a2, Tgif1, Nr2f2, Tead1	Cited2, AR, Hic1, Nr2f2, Tead1
Co-activation	Notch3, Ncoa7, Nr4a2	Cited2
TF PPI	Nfkbia, Bag1	Runx1t1, Hmgb2, Cited2, AR
Other	Mxi1	/

TF: transcription factor.

Table 4. Validation of RNA-Seq results and comparison of selected genes expression between tSKPs and tFBs by qRT-PCR

Gene	Category	RNA-Seq (tSKPs/tFBs) Fold Change	qRT-PCR (tSKPs/tFBs) Fold Change (Mean ± SE)
Mmp9	Up-regulated	9.13	10.87 ± 1.35
Ccl20	Up-regulated	8.14	9.03 ± 0.08
Vcam1	Up-regulated	7.21	6.58 ± 0.50
Csf3	Up-regulated	6.04	5.91 ± 0.31
Cxcl5	Up-regulated	4.96	5.14 ± 1.17
Foxo1	Up-regulated	3.24	3.40 ± 0.39
Nr4a2	Up-regulated	3.92	4.21 ± 0.37
Foxc1	Up-regulated	2.87	2.24 ± 0.35
Foxm1	Down-regulated	2.32	2.38 ± 0.21
Cited2	Down-regulated	1.93	1.71 ± 0.01
Mylk	Down-regulated	4.12	4.18 ± 0.69
Thbs1	Down-regulated	3.16	3.16 ± 0.25
Hmgb2	Down-regulated	1.37	1.23 ± 0.03
Dhcr24	Down-regulated	3.64	3.37 ± 0.48
Dhcr7	Down-regulated	4.00	3.90 ± 0.32
Vegfc	Down-regulated	2.07	2.12 ± 0.05
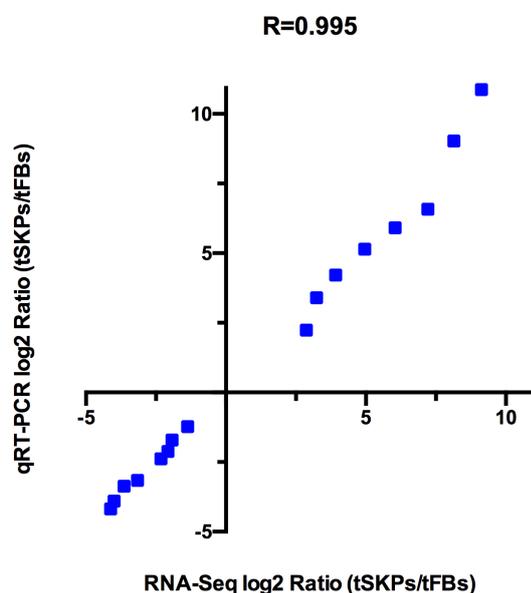
R=0.995

Figure 6. Correlation of selected genes between RNA-Seq and qRT-PCR. Pearson correlation coefficient ($R = 0.995$) was used to determine the consistency in gene expression pattern between RNA-Seq and qRT-PCR.

3.7. qRT-PCR for Data Validation

Sixteen main DEGs (up-regulated: Mmp9,Ccl20, Vcam1, Csf3, Cxcl5, Foxo1, Nr4a2 and Foxc1; down-regulated: Foxm1, Cited2, Mylk, Thbs1, Hmgb2, Dhcr24, Dhcr7 and Vegfc) related to TF or involved in important KEGG pathways were selected to verify the RNA-Seq data by qRT-PCR (Table 4). Pearson correlation coefficient between RNA-Seq data and qRT-PCR data was 0.995 (Figure 6), which indicated that RNA-Seq could provide reliable data for mRNA differential expression analysis.

3.8. RNA-Seq Analysis of tFBs and pFBs

The genomic profiles of tFBs and pFBs from same human dermis sample were also compared by RNA-Seq.

A total of 268 DEGs were identified between pFBs and tFBs, with 139 genes up-regulated and 129 genes down-regulated (Figure 7A). GO function analysis revealed that no significant GO term enriched with DEGs was found (Figure 7B). KEGG pathway enrichment analysis showed that candidate genes were most significantly enriched in the terpenoid backbone biosynthesis, ECM-receptor interaction, focal adhesion and steroid biosynthesis (Figure 7C), most of which were associated with metabolism and morphogenesis.

4. Discussion

In present study, we compared the transcriptional profiles of human tSKPs and tFBs by RNA-Seq. RNA-Seq is an application of next-generation sequencing technique to analyze transcriptome at a given moment and can be used for revealing different gene expression among different samples (*16-18*). RNA-Seq is widely used for laboratory research and clinical studies now, because it provides a more accurate measurement of levels of transcripts and their isoforms over other methods such as microarrays (*19*). To the best of our knowledge, this is the first article performing transcriptomic comparison between tSKPs and tFBs in human.

A total of 1042 genes were found to be differentially expressed between tSKPs and tFBs. Compared with the results of mouse counterpart (*13*), the amount of DEGs is slightly smaller, which indicates that the molecular mechanism underlying differentiation process from SKPs to fibroblasts is not completely same between different species. GO is a common classification scheme for gene function which provides an up-to-date, comprehensive, comparable descriptions of homologous gene and protein sequence across the phylogenetic spectrum (*20,21*). GO functional enrichment reflects the candidate genes are significantly enriched in multiple cellular functions, including cellular component,
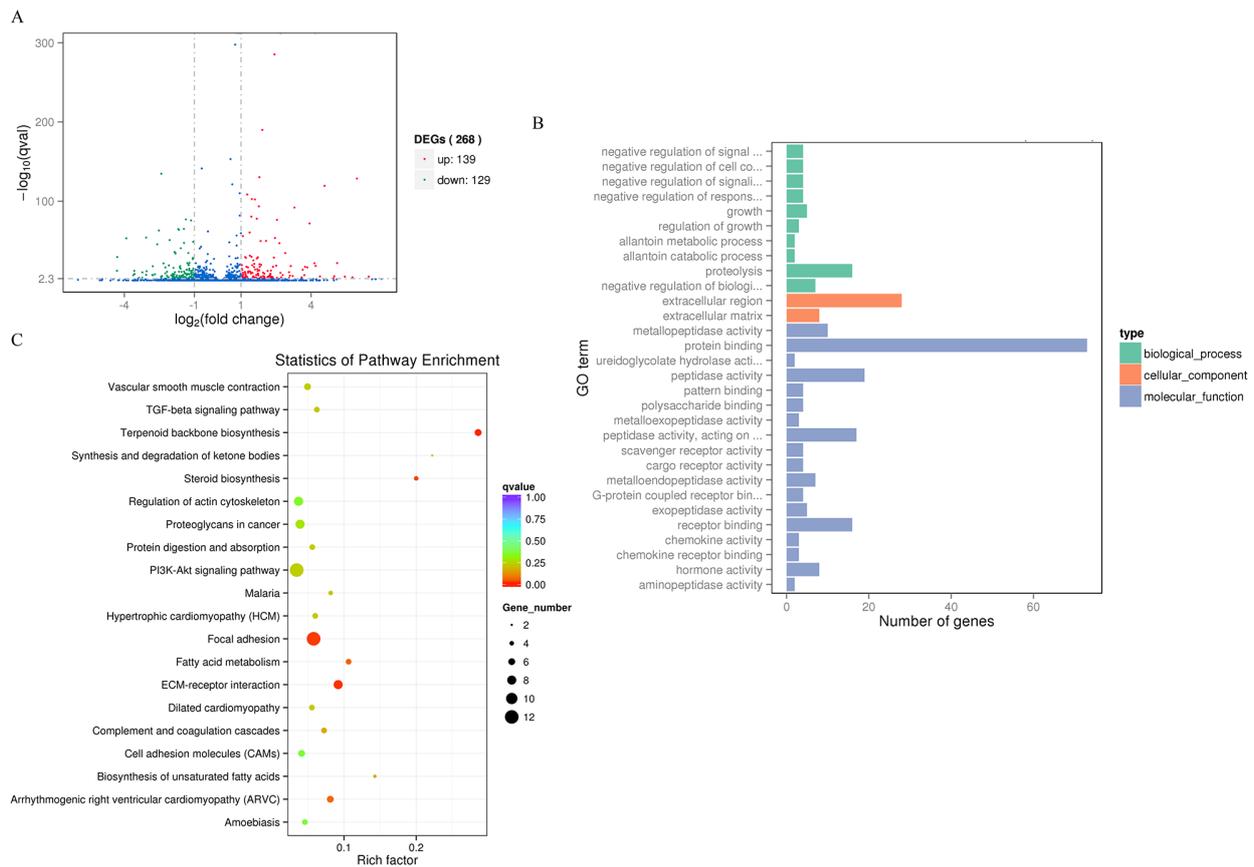
Figure 7. Results of RNA-Seq between pFBs and tFBs. (**A**) Scattered plot of DEGs. (**B**) GO terms of DEGs. *Significantly enriched GO term. (**C**) Scattered plot of DEGs enriched KEGG pathways.

molecular function and biological process. In this study, GO analysis of DEGs showed that these genes were mostly enriched in cell growth, extracellular region, protein binding, peptidase activity and chemokine activity, indicating complex mechanisms were involved in the differentiation of tSKPs towards tFBs.

KEGG analysis detects the pathways where the target genes are most significantly enriched. The result of KEGG identified four major developmental signaling pathways, including TNF signal pathway, focal adhesion, ECM-receptor interaction, and PI3K-Akt signaling pathway. The TNF protein superfamily affects a range of cell biological phenomena, including immune regulation, inflammation, proliferation and differentiation (*22*). In this pathway, tSKPs *vs.* tFBs up-regulated 25 DEGs and down-regulated 5 DEGs (tFBs *vs.* tSKPs up-regulated 5 DEGs and down-regulated 25 DEGs conversely). Numerous studies reported the TNF family is closely related to biological functions of stem cells. TNFα can promote mesendodermal lineage differentiation of mesenchymal stem cells *via* induction of NF-κB, such as myofibroblast (*23*), and osteocytes (*24,25*). The regulation of TNF signaling pathway may play an important role in the transition from tSKPs to fibroblasts. The focal adhesion pathway affects biological processes of cell motility, proliferation and differentiation (*26*). In the focal adhesion, tSKPs

vs. tFBs up-regulated 20 DEGs and down-regulated 23 DEGs (tFBs *vs.* tSKPs up-regulated 23 DEGs and down-regulated 20 DEGs conversely), indicating the differentiation process from tSKPs to tFBs involves the regulation of focal adhesion pathway. The ECM consists of a complex mixture of structure and functional macromolecules that serves as an essential role in tissue and organ morphogenesis (*27*). In ECM-receptor interaction signaling, tSKPs *vs.* FBs up-regulated 14 DEGs and down-regulated 5 DEGs (tFBs *vs.* tSKPs up-regulated 5 DEGs and down-regulated 14 DEGs conversely), which indicated specific interactions occurred between cells and extracellular environment during the differentiation activity of tSKPs and tFBs. The PI3K-Akt signaling pathway is an intracellular signaling pathway that regulates many aspects of cellular functions, including transcription, growth, proliferation, metabolism and survival (*28*). In our study, tSKPs *vs.* tFBs up-regulated 31 DEGs and down-regulated 19 DEGs (tFBs *vs.* tSKPs up-regulated 19 DEGs and down-regulated 31 DEGs conversely). PI3K activation phosphorylates and activates Akt, which is recruited to the plasma membrane along with PI3K-dependent kinase-1 (*29*). Akt can phosphorylate many target proteins, most notably the forkhead box O (FOXO) (*30*), glycogen synthase kinase 3 (GSK3) (*31*), cell cycle regulators p21 and p27 (*31*) and target of

rapamycin (mTOR) (*32*), which explains its relatively wide effects on cell function (*33*). In many cancers, the pathway is well defined in context of tumorigenesis. However, recent studies have highlighted that the pathway is also important for development and cellular differentiation of adult stem cell (*33*). Studies using kinase inhibitors and genetic approaches have shown that both human embryonic stem cells (ESCs) and mouse ESCs require active PI3K/AKT signaling to maintain their undifferentiated properties (*34,35*). Under culture condition conducive for both naive and primed human pluripotent stem cells (PSCs) propagation, high level of PI3K/Akt signaling acts to maintain pluripotency while preventing aberrant differentiation (*36*). Specification of neuro-differentiation requires the sustained status of PI3K/Akt/mTOR signaling (*37*). However, inhibition of this signaling in PSCs promotes the specification of mesoderm differentiation (*38,39*). Under cultured condition permissive for differentiation, the alleviation of PI3K/Akt/mTOR-mediated inhibition of activin/Smad2/3 and Wnt/β-catenin pathways drives PSCs to differentiate into mesendodermal fates (*40*). Therefore, the PI3K/Akt signaling has negative effect on mesodermal differentiation while presenting positive effect on neural differentiation. tSKPs are reported for similar properties as neural stem cells, and tFBs present the function of mesodermal fibroblasts. The KEGG analysis revealed that PI3K/Akt signaling was mostly enriched by down-regulated DEGs when differentiating tSKPs into tFBs. Therefore, we assume that PI3K/Akt signaling may be important in the differentiation process from tSKPs to tFBs and the regulation of PI3K/Akt signaling may activate tSKPs differentiation.

TFs regulate gene expression by binding to specific upstream nucleotide sequences to achieve biological functions. Analysis of TFs between tSKPs and tFBs may also help us lift the veil on the transition from tSKPs and FBs. Among the TFs down-expressed in tFBs, many genes have been reported to encode for functions in the neural system. Nr4a2 is associated with neuron progenitors and neurogenesis of hippocampus neural stem cells (*41,42*). The Klf family can promotes self-renewal and cellular programing of stem cells (*43*). Snail2 involves in the regulation of neural crest development (*44*). Inhibiting the expression of the above genes in tFBs, which are related to neural system, may be important for tSKPs differentiation into mesodermal lineages rather than neural cells. Ceg1 is highly expressed in both embryonic and adult heat, which is required for differentiation of mouse embryonic cell into cardiomyocytes and the formation of cohesive myocardium-like structure in a cell-autonomous fashion (*45*). Tgif1 has been showed to regulate quiescence and self-renewal of hematopoietic stem cells (*45*). Silencing of Tgif1 in tendon-derived stem cells can improve the tendon-to-bone insertion site regeneration (*46*). Cdkn1a (alternatively p21), Foxo1 (*47*) and Foxc1 (*8*) are key

multifunctional downstream signaling nodes of PI3K/Akt signaling. The down-regulation of above genes in tFBs suggests the inhibition of PI3K/Akt signaling may involve in the process of transition from tSKPs to tFBs, which was consistent with the results of KEGG. Among the TFs up-expressed in tFBs, Foxm1 is a proliferation-associated TF, which stimulates cell cycle progression by promoting the entry into S-phase and M-phase (*49*). The knockout of Foxm1 in mice is lethal with defective development of heart, lung and liver (*49*). Thus, Foxm1 is essential for the maintenance of genomic stability and chromosome integrity. Thbs1, a transient component of extracellular matrix in developing and repairing tissue, functions as a cell adhesion molecule and modulates cell movement and cell proliferation (*9*). Thbs1 has been shown to be involved in the activation of latent transforming growth factor (TGF) β (*50*). The up-regulation of Thbs1 indicates that it may associate with the formation process of tFBs through TGFβ signaling pathway.

A further comparison of tFBs and pFBs identified 268 DEGs. Compared with the results of tSKPs and tFBs, the amount of DEGs was much smaller. In addition, no GO term was significantly enriched by DEGs and KEGG analysis revealed only few pathways related to metabolism and morphogenesis were enriched by DEGs. The comparative transcriptome analysis of two fibroblasts suggested that no major difference of biological function was found between tFBs and pFBs.

In conclusion, we compared the transcriptional profiles between tSKPs and tFBs by RNA-Seq. Our studies showed that the up-regulated and down-regulated genes were significantly enriched in TNF signaling pathway, focal adhesion, ECM-receptor interaction and PI3K/Akt signaling pathway. A further TF analysis of DEGs revealed that the down-expressed TFs (p21, Foxo1and Foxc1) in tFB were the downstream nodes of PI3K-Akt signaling pathway, which suggested PI3K-Akt signaling pathway might play an important role in tSKPs differentiation. The results of our study are useful for investigating the molecular mechanisms in tSKPs differentiation into tFBs, making it possible to take advantage of their potential application in regenerative medicine.

Acknowledgements

References

1. Toma JG, Akhavan M. Isolation of multipotent adult stem cells from the dermis of mammalian skin. Nat Cell Biol.

2001; 3:778-784.

2. Dai R, Hua W, Xie H, Chen W, Xiong L, Li L. The human skin-derived precursors for regenerative medicine: current state, challenges, and perspectives. Stem Cells Int. 2018; 2018:8637812.

3. Biernaskie JA, McKenzie IA, Toma JG, Miller FD. Isolation of skin-derived precursors (SKPs) and differentiation and enrichment of their Schwann cell progeny. Nat Protoc. 2007; 1:2803-2812.

4. Toma JG, Mckenzie IA, Bagli D, Miller FD. Isolation and characterization of multipotent skin-derived precursors from human skin. Stem Cells 2005; 23:727-737.

5. Fernandes KJL, McKenzie IA, Mill P, Smith KM, Akhavan M, Barnabé-Heider F, Biernaskie J, Junek A, Kobayashi NR, Toma JG, Kaplan DR, Labosky PA, Rafuse V, Hui CC, Miller FD. A dermal niche for multipotent adult skin-derived precursor cells. Nat Cell Biol. 2004; 6:1082-1093.

6. Dai R, Hua W, Chen W, Xiong L, Li L, Li Y. Isolation, characterization, and safety evaluation of human skin-derived precursors from an adherent monolayer culture system. Stem Cell Int. 2019; 2019:9194560.

7. Hill RP, Gledhill K, Gardner A, Higgins CA, Crawford H, Lawrence C, Hutchison CJ, Owens WA, Kara B, James SE, Jahoda CAB. Generation and characterization of multipotent stem cells from established dermal cultures. PLoS One. 2012; 7:e50742.

8. Wenzel V, Roedl D, Gabriel D, Gordon LB, Herlyn M, Schneider R, Ring J, Djabali K. Naive adult stem cells from patients with Hutchinson-Gilford progeria syndrome express low levels of progerin *in vivo*. Biol Open. 2012; 1:516-526.

9. Biernaskie J, Miller FD. Skin-derived precursors(SKPs): *in vivo* cell fate is limited to the neural crest lineage, and is determined by tissue-specific factors. Int J Dev Neruoscience. 2006; 24:495-603.

10. Biernaskie J, Paris M, Morozova O, Fagan BM, Marra M, Pevny L, Miller FD. SKPs derived from hair follicle precursors and exhibit properties of adlut dermal stem cells. Cell Stem Cell. 2009; 5:610-623.

11. Fushan AA, Turanov AA, Lee S, Kim EB, Lobanov AV, Yim SH, Buffenstein R, Lee S, Chang K, Rhee H, Kim J, Yang K, Gladyshev VN. Gene expression defines natural changes in mammalian lifespan. Aging Cell. 2015; 14:352-365.

12. Fulton DL, Sundararajan S, Badis G, Hughes TR, Wasserman WW, Roach JC, Sladek R. TFCat : the curated catalog of mouse and human transcription. Genome Biol. 2009; 10:R29.

13. Mao Y, Xiong L, Wang S, Zhong J, Zhou R, Li L. Comparison of the transcriptomes of mouse skin derived precursors (SKPs) and SKP-derived fibroblasts (SFBs) by RNA-Seq. PLoS One. 2015; 10:e0117739.

14. Zhao M, Whitworth KM, Zhang X, Zhao J, Miao Y, Zhang Y, Prather RS. Deciphering the mesodermal potency of porcine skin-derived progenitors (SKP) by microarray analysis. Cell Reprogram. 2010; 12:161-173.

15. Vaquerizas JM, Kummerfeld SK, Teichmann SA, Luscombe NM. A cesus of human transcription factors: function, expression and evolution. Nat Rev Genet. 2009; 10:252-263.

16. Chu Y, Corey DR. RNA sequencing : platform selection, experimental design, and data interpretation. Nucleic Acid Ther. 2012; 22:271-274.

17. Wilhelm BT, Landry J. RNA-Seq-quantitative measurement of expression through massively parallel RNA-sequencing. Methods. 2009; 48:249-257.

18. Wang Z, Gerstein M, Snyder M. RNA-Seq : a revolutionary tool for transcriptomics. Nat Rev Genet. 2009; 10:57-63.

19. Fu X, Fu N, Guo S, Yan Z, Xu Y, Hu H, Menzel C, Chen W, Li Y, Zeng R, Khaitovich P. Estimating accuracy of RNA-Seq and microarrays with proteomics. BMC Genomics. 2009; 10:161.

20. Michael A, Catherine A B, Judith A B, *et al*. Gene Ontology : tool for the unification of biology. The Gene Ontology Consortium. Nat Commun. 2000; 25:25-29.

21. The Gene Ontology Consortium. The Gene Ontology Resource: 20 years and still GOing strong. Nucleic Acids Res. 2019; 47:D330-D338.

22. Sabio G, Davis RJ. TNF and MAP kinase signaling pathways. Semin Immunol. 2014; 26:237-245.

23. Zhou J, Ma T, Cao H, Chen Y, Wang C, Chen X, Xiang Z, Han X. TNF-α-induced NF-κB activation promotes myofibroblast differentiation of LR-MSCs and exacerbates bleomycin-induced pulmonary fibrosis. J Cell Physiol. 2018; 233:2409-2419.

24. Feng X, Feng G, Xing J, Shen B, Li L, Tan W, Xu Y, Liu S, Liu H, Jiang J, Wu H, Tao T, Gu Z. TNF-α triggers osteogenic differentiation of human dental pulp stem cells *via* the NF-κB signalling pathway. Cell Biol Int. 2013; 37:1267-1275.

25. Kotake S, Nanke Y. Effect of TNFα on osteoblastogenesis from mesenchymal stem cells. Biochim Biophsica Acta. 2014; 1840:1209-1213.

26. Mathieu PS, Loboa EG. Cytoskeletal and focal adhesion influences on mesenchymal stem cell shape, mechanical properties, and differentiation down osteogenic, adipogenic, and chondrogenic pathways. Tissue Eng Part B Rev. 2012; 18:436-444.

27. Rozario T, Desimone DW. The extracellular matrix in development and morphogenesis: a dynamic view. Dev Biol. 2010; 341:126-140.

28. Vanhaesebroeck B, Stephens L, Hawkins P. PI3K signalling: the path to discovery and understanding. Nat Publ Gr. 2012; 13:195-203.

29. Vanhaesebroeck B, Guibert JG, Graupera M. The emerging mechanisms of isoform-specific PI3K signalling. Nat Rev Mol Cell Biol. 2010; 11:329-341.

30. Kops GJ, de Ruiter ND, De Vries-Smits AM, Powell DR, Bos JL, Burgering BM. Direct control of the Forkhead transcription factor AFX by protein kinase B. Nature. 1999; 398:630-634.

31. Cross DE, Alessi DR, Cohen P, Andjelkovich M, Hemmings BA. Inhibition of glycogen synthase kinase-3 by insulin mediated by protein kinase B. Nature. 1995; 378:785-789.

32. Jacinto E, Facchinetti V, Liu D, Soto N, Wei S, Jung SY, Huang Q, Qin J, Su B. SIN1/MIP1 maintains rictor-mTOR complex integrity and regulates Akt phosphorylation and substrate specificity. Cell. 2006; 127:125-137.

33. Yu JSL, Cui W. Proliferation, survival and metabolism: the role of PI3K/AKT/mTOR signalling in pluripotency and cell fate determination. Deveopment. 2016; 143:3050-3060.

34. Paling NRD, Wheadon H, Bone HK, Welham MJ. Regulation of embryonic stem cell self-renewal by phosphoinositide 3-kinase-dependent signaling. J Biol Chem. 2004; 279:48063-48070.

35. Kingham E, Welham M. Distinct roles for isoforms of

the catalytic subunit of class-IA PI3K in the regulation of behaviour of murine embryonic stem cells. J Cell Sci. 2009; 122:2311-2321.

36. Betschinger J, Nichols J, Dietmann S, Corrin PD, Paddison PJ, Smith A. Exit from pluripotency is gated by intracellular redistribution of the bHLH transcription factor Tfe3. Cell. 2013; 153:335-347.

37. Fishwick KJ, Li RA, Halley P, Deng P, Storey KG. Initiation of neuronal differentiation requires PI3-kinase/TOR signalling in the vertebrate neural tube. Dev Biol. 2010; 338:215-225.

38. McLean AB, D'Anour KA, Jones KL, Krishnamoorthy M, Kulik MJ, Reynolds DM, Sheppard AM, Liu H, Xu Y,Baetge EE, Dalton S. Activin a efficiently specifies definitive endoderm from human embryonic stem cells only when phosphatidylinositol 3-kinase signaling is suppressed. Stem Cells. 2007; 25:29-38.

39. Zhou J, Su P, Wang L, Chen J, Zimmermann M, Genbacev O, Afonja O, Horne MC, Tanaka T, Duan E, Fisher SJ, Liao J, Chen J, Wang F. mTOR supports long-term self-renewal and suppresses mesoderm and endoderm activities of human embryonic stem cells. Proc Natl Acad Sci U S A. 2009; 106:7840-7845.

40. Yu JSL, Ramasamy TS, Murphy N, Holt MK, Czapiewski R, Wei SK, Cui W. PI3K/mTORC2 regulates TGF-β/Activin signalling by modulating Smad2/3 activity *via* linker phosphorylation. Nat Commun. 2015; 6:7212.

41. Shao CZ, Xia KP. Sevoflurane anesthesia represses neurogenesis of hippocampus neural stem cells *via* regulating microRNA-183-mediated NR4A2 in newborn rats. J Cell Physiol. 2019; 234:3864-3873.

42. Chen S, Luo GR, Li T, Liu TX, Le W. Correlation of Nr4a2 Expression with the Neuron Progenitors in Adult Zebrafish Brain. J Mol Neurosci. 2013; 51:719-723.

43. Bialkowska AB, Yang VW, Mallipattu SK. Krüppel-like factors in mammalian stem cells and development. Deveopment. 2017; 144:737-754.

44. Tien CL, Jones A, Wang H, Gerigk M, Nozell S, Chang C. Snail2/Slug cooperates with Polycomb repressive complex 2 (PRC2) to regulate neural crest development. Deveopment. 2015; 142:722-731.

45. Liu J, Qi Y, Li S, Hsu SC, Saadat S, Hsu J, Rahimi SA, Lee LY, Yan C, Tian X, Han Y. CREG1 Interacts with Sec8 to promote cardio-myogenic differentiation and cell-cell adhesion. Stem Cells. 2016; 34:2648-2660.

46. Chen L, Jiang C, Tiwari SR, Shrestha A, Xu P, Liang W, Sun Y, He S, Cheng B. TGIF1 gene silencing in tendon-derived stem cells improves the tendon-to-bone insertion site regeneration. Callular Physilogy Biochem. 2015; 37:2101-2114.

47. Paradis S, Ruvkun G. Caenorhabditis elegans Akt / PKB transduces insulin receptor-like signals from AGE-1 PI3 kinase to the DAF-16 transcription factor. Genes Dev. 1998; 12:2488-2498.

48. Yu Z, Xu H, Wang H, Wang Y. Foxc1 promotes the proliferation of fibroblast-like synoviocytes in rheumatoid arthritis *via* PI3K/AKT signalling pathway. Tissue Cell. 2018; 53:15-22.

49. Wierstra I. The transcription factor FOXM1 (Forkhead box M1): proliferation-specific expression, transcription factor function, target genes, mouse models, and normal biological roles. Adv Cancer Res. 2013; 118:97-398.

50. Murphy-ullrich JE, Poczatek M. Activation of latent TGF-β by thrombospondin-1: mechanisms and physiology. Cytokine Growth Factor Rev. 2000; 11:59-69.

§These authors contributed equally to this work.
Address correspondence to:
Li Li, Department of Dermatology, West China Hospital, Sichuan University, No. 37, Guo Xue Xiang, Chengdu, 610041, China
E-mail: hxskincos2017@qq.com